References

[1]Chow, L. C. and Parish, R. C., "Condensation Heat Transfer in a Microgravity Environment," AIAA Paper 86-0068, Jan. 1986.

[2]Seban, R. A. and Hodgson, J. A., "Laminar Film Condensation in a Tube with Upward Vapor Film," *International Journal of Heat and Mass Transfer*, Vol. 25, 1982, pp. 1291-1300.

[3]Henstock, W. H. and Hanratty, T. J., "The Interfacial Drag and the Height of the Wall Layer in Annular Flows," *AIChE Journal*, Vol. 22, 1976, pp. 990-1000.

Fluid Loss from a Puncture of a Space Radiator

D. E. Tilton* and L. C. Chow†
University of Kentucky, Lexington, Kentucky

Introduction

FUTURE space missions will require the development of lightweight, large surface area radiators capable of rejecting large quantities of waste heat. A lightweight expandable bellow radiator has been suggested for this purpose.[1] Unlike radiators with rigid structures, this radiator is only exposed to the space environment when it is in operation. Even so, the susceptibility of the radiator to damage from micrometeoroids must be evaluated. These tiny particles travel through space at an average velocity of approximately 20 km/s. Since the radiator is lightweight and flexible, it is likely that punctures will occur. No previous research has been conducted to determine the mass loss of the radiator working fluid associated with the puncture of a bellow in a space environment. The present experiment was designed to simulate this situation so that the extent of potential damage and the effects on radiator performance could be evaluated.

Experimental Apparatus and Procedures

The experimental apparatus was designed to simulate puncture conditions for a flexible radiator. The test section consisted of a 3800-cc, double-walled, stainless-steel vessel with a membrane holder on the bottom. The test section was located in an evacuated bell jar. Either superheated steam (superheated steam case) or saturated steam with a condensate layer covering the membrane (condensate case) occupied the test section. The other side of the membrane was exposed to the near-vacuum environment of the bell jar. The temperature in the test section was controlled by circulating constant temperature water through the test section double wall. The membrane was punctured using a solenoid activated needle. The pressure and temperature inside the test section were monitored as a function of time after puncture. For a more detailed experimental description, see Ref. 2.

The mass loss rate for the condensate case is calculated by estimating the time it took for the entire condensate layer to leak out. Data required to compute the mass loss rates in this manner are given in Table 1, where T_{sat} is the saturation temperature, V_{add} is the volume of liquid added to the test section, and t is the estimated time it took to expel the entire layer of condensate. It is assumed that the temperature within the test section is uniform at saturation. The proper amount of water was added using a calibrated syringe. The high uncertainty in time is due to the difficulty in observing when all the condensate was expelled.

The mass loss rate for the superheated steam case is calculated by estimating the amount of mass in the test section just prior to puncture and at the end of the run. The difference is then divided by the time of the run. Since the volume of the test section is constant, the mass at each time can be calculated if the temperatures and pressures are known. Data collected for this case are given in Table 2. T_1 and P_1 are the temperature and pressure just prior to puncture. T_2 and P_2 are the temperature and pressure recorded t s after puncture. The time t for this case was determined by the pressure rise in the bell jar, which was read from the pressure thermocouple gage in the vacuum test machine. The time is measured using the strip chart recorder. As soon as the bell jar pressure rises above 1.0 mm Hg, the test is ended. If the test were run longer, the mass-loss rate would begin to decrease significantly due to the pressure drop in the test section.

Mass Loss Rate Determination

Condensate Case

The mass loss rate for the condensate case can be estimated from the experimental data given in Table 1. Since the volume of the test section is constant, an estimate of the mass of the condensate layer can be obtained by the following method. The volume of the test section is divided by the mass of the liquid added to obtain a total specific volume. This value, along with the specific volumes of the vapor and liquid corresponding to the recorded saturation temperature, is used to calculate the quality of the mixture and mass of the condensate layer. The mass loss rate $\dot{m}$ is obtained by simply dividing condensate mass by the experimentally observed time for the entire layer to be expelled. The resulting mass loss rates for this case are presented in Fig. 1.

The mass loss rate for the condensate case may also be predicted theoretically by using the orifice flow equation.[3] However, this prediction is not quite representative of the experiment due to the irregular puncture areas and irregular discharge observed experimentally. This prediction should only give an order of magnitude value. The mass loss rates calculated from the orifice velocity predictions and the measured puncture areas are approximately 2.5 to 3.0 times less than the experimentally determined values for all runs. The difference is attributed to the fact that the momentum of the liquid flow may have increased the hole area. The puncture areas discussed in the following section were measured after the experiment and with no liquid flowing through the holes.

Superheated Steam Case

To calculate the mass loss rate for the superheated steam case, the values for mass contained in the test section at the beginning and end of the run were computed using the ideal gas law. Superheated steam in the present pressure and temperature range behaves like an ideal gas, that is, the compressibility factor Z is approximately 1.0. The difference in these two values was divided by the time of the run to give the mass loss rate. The mass loss rates calculated in this manner from the data in Table 2 are plotted against the puncture areas. The slope is the average mass flux. This is shown in Fig. 2.

The mass flux for this case can be predicted theoretically using the choked flow equation.[4] The average experimental

Received April 10, 1986; presented as Paper 86-1324 at the AIAA/ASME 4th Thermophysics and Heat Transfer Conference, Boston, MA, June 2-4, 1986; revision received July 14, 1986.

*Research Assistant, Mechanical Engineering Department. Student Member AIAA.

†Associate Professor, Mechanical Engineering Department. Member AIAA.

Table 1 Condensate case data

Run	T_{sat}, °C ±0.5	V_{add}, cm³ ±0.2	t, s ±1.0
1	70.2	5.1	5.6
2	67.8	5.1	5.4
3	68.6	6.3	6.0
4	66.8	7.0	6.0

Table 2 Superheated steam case data

Run	T_1, °C ±0.5	P_1, kPa ±0.2	T_2, °C ±0.5	P_2, kPa ±0.2	t, s ±0.3
5	70.2	21.7	68.6	21.0	62.0
6	68.2	20.0	67.4	19.2	20.5
7	71.0	18.3	70.2	16.9	26.0
8	70.8	20.0	69.6	19.0	8.5
9	70.4	22.2	69.4	20.5	7.3
10	70.2	20.5	68.6	17.7	7.5
11	70.2	21.1	69.4	19.4	3.0

Table 3 Puncture and needle area data

Run	Material[a]	A_n, mm²	A, mm²	A_n/A
1	C	0.114	0.029	3.93
2	C	0.257	0.036	7.14
3	C	0.114	0.046	2.48
4	A	0.257	0.050	5.14
5	C	0.114	0.008	14.25
6	A	0.257	0.026	9.88
7	A	0.621	0.039	15.92
8	A	0.456	0.080	5.70
9	C	0.881	0.172	4.72
10	A	1.267	0.221	5.73
11	A	2.011	0.370	5.43

[a]A = aluminum film-plastic laminate, C = clear plastic laminate.

mass flux of 0.125 kg/h mm² and the theoretically determined value of 0.122 kg/h mm² were in excellent agreement.

Membrane Puncture

For the two experimental cases discussed, two different membrane materials were tested. One was a clear plastic laminate 0.152 mm thick. The other was a plastic-aluminum film laminate 0.137 mm thick. Table 3 lists material type, actual hole area A, needle cross-sectional area A_n, and the area ratio A_n/A. Due to the wide variation in the area ratio, no correlation can be made between needle size and puncture area for the two materials tested. An existing correlation for thin metal sheets was shown to be invalid for the flexible membrane materials as expected.[5]

Photographs (presented in Ref. 2) of the different punctures taken with an electron microscope show the differences in puncture between the two different membrane materials. The clear plastic laminate stretched more readily and the puncture was fairly clean and round. The other material ripped when the needle was forced through. The irregular hole shapes made area calculation difficult. The area of the puncture shown in the photographs was estimated using a grid. This value was then reduced by the magnification factor to determine the actual puncture area. The error associated with this calculation is estimated to be less than 10%.

Conclusions and Recommendations

This research provides estimates of mass loss rates for two cases, which can be used to determine the mass loss of the radiator fluid associated with micrometeoroid puncture. The mass loss rates for the superheated steam case are very low. The experiment shows that these rates can be accurately predicted by the choked flow equation. The mass loss rates for the condensate case were on the order of 1000 times greater than the superheated steam case. The thickness of the condensate layer should be minimized to reduce mass loss and resistance to heat transfer. It is also necessary to develop a correlation to predict the clear hole area for a given membrane material, micrometeoroid size, and velocity. A correlation of this type could be used in conjunction with micrometeoroid flux data to predict the mass loss rates for any projected radiator size, type, and duty cycle.

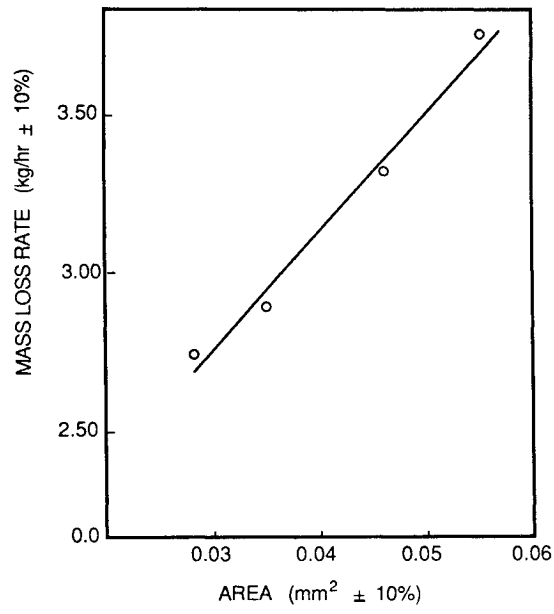

Fig. 1 Condensate case results.

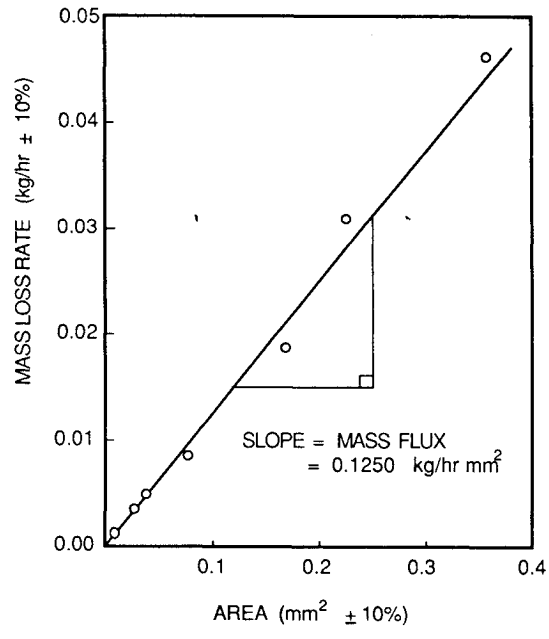

Fig. 2 Superheated steam case results.

Acknowledgments

The research was funded by the Air Force Office of Scientific Research under Contract F49620-82-C-0035. The research was conducted at Washington State University, Pullman, Washington.

References

[1]Chow, L. C., Mahefkey, E. T., and Yokajty, J. E., "Low Temperature Expandable Megawatt Pulse Power Radiator," *Journal of Spacecraft and Rockets,* Vol. 23, Sept.-Oct. 1986, pp. 539-541.

[2]Tilton, D. E. and Chow, L. C., "Flow Through a Pierced Membrane in a Vacuum," AIAA Paper 86-1324, June 1986.

[3]Oswatitsch, K. and Kuerti, G., *Gas Dynamics,* Academic Press, New York, 1956, p. 51.

[4]Robertson, J. A. and Crowe, C. T., *Engineering Fluid Mechanics,* 2nd Ed., Houghton Mifflin Company, Boston, 1980, p. 532.

[5]*Meteoroid Damage Assessment,* NASA SP-8042, 1970.

Radiative Shape Factors Between Differential Ring Elements on Concentric Axisymmetric Bodies

Michael F. Modest*
The Pennsylvania State University
University Park, Pennsylvania

Nomenclature

dA_i	= area of differential ring element
B	= function defined by Eq. (9)
dF_{d1-d2}	= infinitesimal radiation shape factor from differential element dA_1 to dA_2
ds_i	= width of differential ring element $dA_i = 2\pi r_i ds_i$
r,r_1,r_2	= radius (of element 1 and 2, respectively)
$R_i(z),R_o(z)$	= local radius of inner and outer axisymmetric body
S	= distance between two points on dA_1 and dA_2
z,z_1,z_2	= axial position of element 1 and 2, respectively
α_{12}	= function defined by Eq. (6)
β_i	= angle between surface normal to dA_i and point-connection line S
θ,θ_1,θ_2	= tilt angle of surface with respect to z-axis
$\psi,\psi_{min},\psi_{max}$	= (minimum or maximum) azimuth angle with which strip dA_2 is seen from a point on dA_1
ϕ_1,ϕ_2	= function defined by Eq. (6)
Γ_i,Γ_o	= minimum and maximum permissible values for $\cos\psi$ based on interfering surface between any two differential ring elements

Introduction

LARGE amounts of radiative shape factors have been published in the past, in particular during the 1960's, many in the form of formulas, some in the form of computer calculations and graphs. A good review on published shape factors has been given by Siegel and Howell[1] and Howell[2]. An analytical formula has been given by Morizumi[3] for a simple paraboloidal surface, while some numerical calculations have been carried out by Robbins and Todd[4] for a single axisymmetric body. Chung and Naraghi[4,5] formulated shape factor expressions between a sphere and a number of axisymmetric bodies, while Masuda[7] treated the case of circular-finned cylinders. It is the purpose of this paper to add working formulas for shape factors between two ring strip elements on two arbitrarily shaped concentric axisymmetric bodies.

Analysis

Figure 1 shows a schematic of the plasma chamber of the NET (next European torus) fusion reactor as an example for two concentric axisymmetric bodies. Consider two infinitesimal bands ds_1 and ds_2, as indicated in Fig. 1 for the case that ds_1 lies on the outer axisymmetric body, while ds_2 lies on the inner one. The shape factor between them may be evaluated as[1]

$$dF_{d1\to d2} = \frac{2}{\pi}\int_{\psi_{min}}^{\psi_{max}} \frac{\cos\beta_1 \cos\beta_2}{S^2}\, d\psi\, r_2\, ds_2 \tag{1}$$

where symmetry with respect to the azimuthal angle ψ has been incorporated. Here, S is the distance between two points on the bands, β_i the angle between the surface normal of ds_i and the vector to the point on the other band, ψ the azimuthal angle between the two points (in the plane perpendicular to the rotation axis), and ψ_{min} and ψ_{max} the limiting angles with which the band ds_2 is seen from a point on ds_1. To clarify the meaning of the limiting angles ψ_{min} and ψ_{max}, Fig. 2 shows vertical and horizontal cuts through the concentric axisymmetric bodies depicted in Fig. 1. The locations of dA_1 and dA_2 have been changed a bit in order to show certain shading effects. For $\psi = 0$, a vector from dA_1 to dA_2 would intersect A_1 itself before getting to dA_2. Thus, there is a minimum azimuthal angle ψ_{min} at which the vector will just graze by the corner at A_1. If there were no inner cylinder ψ_{max} would be determined by the range of ψ over which $\cos\beta_1$ and $\cos\beta_2$ would remain positive (e.g., $\psi_{max} = \pi$ for a horizontal ring and $\psi_{max} = \cos^{-1}(r_2/r_1)$ for a vertical ring). With an inner cylinder present, a vector from dA_1 to dA_2 with an azimuthal angle larger than the one labeled $\cos^{-1}\Gamma_i$ would intersect the inner cylinder before getting to dA_2. The relevant ψ_{max} would then be the smaller of the two, as indicated in Fig. 2. The integrand in Eq. (1) is readily found from geometric considerations as

$$S^2 = r_1^2 + r_2^2 - 2r_1 r_2 \cos\psi + (z_2 - z_1)^2 \tag{2}$$

$$S\cos\beta_1 = -(r_1 - r_2\cos\psi)\cos\theta_1 - (z_2 - z_1)\sin\theta_1 \tag{3}$$

$$S\cos\beta_2 = (r_1\cos\psi - r_2)\cos\theta_2 + (z_2 - z_1)\sin\theta_2 \tag{4}$$

where θ_i is the angle between the z axis and strip ds_i as indicated in Fig. 2 (measured from the z axis into the outward direction onto the backside of the surface; thus, $\theta = 0$ for a vertical, outward facing strip, $-\pi/2 < \theta < \pi/2$ for outward facing strips, and $\pi/2 < \theta < 3\pi/2$ for inward facing strips). Therefore,

$$\frac{dF_{d1\to d2}}{2\pi r_2 ds_2} = \frac{\cos\theta_1\cos\theta_2}{4\pi^2 r_1 r_2}\int_{\psi_{min}}^{\psi_{max}} \frac{(\phi_1 - \cos\psi)(\phi_2 - \cos\psi)}{(\alpha_{12} - \cos\psi)^2}\, d\psi \tag{5}$$

with

$$\phi_i = \frac{r_i}{r_j} + \frac{z_j - z_i}{r_j}\tan\theta_i,\ i=1, j=2, \text{ or } i=2, j=1$$

$$\alpha_{12} = \tfrac{1}{2}\left(\frac{r_1}{r_2} + \frac{r_2}{r_1}\right) + \frac{(z_2 - z_1)^2}{2r_1 r_2} \tag{6}$$

This may be integrated to yield

$$\frac{dF_{d1\to d2}}{2\pi r_2 ds_2} = \frac{\cos\theta_1\cos\theta_2}{4\pi^2 r_1 r_2}[B(\alpha_{12},\phi_1,\phi_2,\cos\psi_{max}) - B(\alpha_{12},\phi_1,\phi_2,\cos\psi_{min})] \tag{7}$$

Received July 15, 1986; revision received Oct. 15, 1986.

*Professor of Mechanical Engineering, Department of Mechanical Engineering.